Plant Mol Biol (2017) 95:463–479
DOI 10.1007/s11103-017-0664-y

Functional characterization of chloroplast-targeted RbgA GTPase in higher plants

Young Jeon[1] · Hee-Kyung Ahn[1] · Yong Won Kang[2] · Hyun-Sook Pai[1]

Received: 15 March 2017 / Accepted: 1 October 2017 / Published online: 16 October 2017

Abstract

Key message **Plant RbgA GTPase is targeted to chloroplasts and co-fractionated with chloroplast ribosomes, and plays a role in chloroplast rRNA processing and/or ribosome biogenesis.**

Abstract Ribosome Biogenesis GTPase A (RbgA) homologs are evolutionarily conserved GTPases that are widely distributed in both prokaryotes and eukaryotes. In this study, we investigated functions of chloroplast-targeted RbgA. *Nicotiana benthamiana* RbgA (NbRbgA) and *Arabidopsis thaliana* RbgA (AtRbgA) contained a conserved GTP-binding domain and a plant-specific C-terminal domain. NbRbgA and AtRbgA were mainly localized in chloroplasts, and possessed GTPase activity. Since *Arabidopsis rbgA* null mutants exhibited an embryonic lethal phenotype, virus-induced gene silencing (VIGS) of *NbRbgA* was performed in *N. benthamiana*. *NbRbgA* VIGS resulted in a leaf-yellowing phenotype caused by disrupted chloroplast development. NbRbgA was mainly co-fractionated with 50S/70S ribosomes and interacted with the chloroplast ribosomal proteins cpRPL6 and cpRPL35. NbRbgA deficiency lowered the levels of mature 23S and 16S rRNAs in chloroplasts and caused processing defects. Sucrose density gradient sedimentation revealed that NbRbgA-deficient chloroplasts contained reduced levels of mature 23S and 16S rRNAs and diverse plastid-encoded mRNAs in the polysomal fractions, suggesting decreased protein translation activity in the chloroplasts. Interestingly, NbRbgA protein was highly unstable under high light stress, suggesting its possible involvement in the control of chloroplast ribosome biogenesis under environmental stresses. Collectively, these results suggest a role for RbgA GTPase in chloroplast rRNA processing/ribosome biogenesis, affecting chloroplast protein translation in higher plants.

Keywords Chloroplast abnormality · *Nicotiana benthamiana* · Ribosomal RNA processing · Ribosome association · Virus-induced gene silencing

Introduction

Ribosome biogenesis is a complex process that is tightly coordinated with cell growth and division. Prokaryotic ribosome biogenesis involves the synthesis, processing, chemical modification, and assembly of three rRNA molecules (23S, 16S, and 5S) and > 50 ribosomal proteins. The assembly maps of 30S and 50S ribosome subunits were constructed through in vitro reconstitution of functional ribosomal particles from individual ribosomal components (Traub and Nomura 1968, 1969; Rohl and Nierhaus 1982; Herold and Nierhaus 1987). More recent evidence suggests that prokaryotic ribosome assembly utilizes multiple parallel

Electronic supplementary material The online version of this article (doi:10.1007/s11103-017-0664-y) contains supplementary material, which is available to authorized users.

✉ Hyun-Sook Pai
hspai@yonsei.ac.kr

Young Jeon
planty@hanmail.net

Hee-Kyung Ahn
hkyungahn88@yonsei.ac.kr

Yong Won Kang
alpower96@naver.com

[1] Department of Systems Biology, Yonsei University, Seoul 03722, South Korea

[2] R&D Center, Morechem Co., Ltd., Yongin, Gyeonggi-do 16954, South Korea

pathways instead of following a single pathway (Talkington et al. 2005; Adilakshmi et al. 2008; Sykes and Williamson 2009). Chloroplasts are thought to have originated from the endosymbiosis of a photosynthetic prokaryotic ancestor into a eukaryotic host. Chloroplasts have their own genome and machinery for gene transcription and translation, including chloroplast ribosomes. Chloroplast rRNAs are highly conserved in their sequences and are most closely related to eubacterial rRNAs (Tiller and Bock 2014). Proteomic studies have shown that chloroplast ribosomes from higher plants have total 58 ribosomal proteins and possess orthologs to all 52 ribosomal proteins of *Escherichia coli* except RPL25 and RPL30 (Yamaguchi and Subramanian 2000, 2003; Sharma et al. 2007; Tiller and Bock 2014). Chloroplast ribosomal proteins are generally larger than their *E. coli* counterparts, and furthermore, chloroplast ribosomes possess five plastid-specific ribosomal proteins (PSRPs). Electron cryomicroscopy has revealed that the overall structure of chloroplast ribosomes is similar to that of prokaryotic 70S ribosomes, but chloroplast ribosomes are larger and have special features including PSRPs, suggesting the evolution of a specific ribosome structure to facilitate the translation of chloroplast mRNAs (Manuell et al. 2007; Sharma et al. 2007; Ahmed et al. 2016).

Ribosome biogenesis is assisted by many assembly factors, including the universally conserved GTPases (Caldon and March 2003; Verstraeten et al. 2011). Chloroplasts have homologs of bacterial GTPases that play a crucial role in prokaryotic ribosome biogenesis, although only a few chloroplast GTPases have been characterized so far. Rice OsNOA1/RIF1, a homolog of bacterial YqeH, encodes a chloroplast GTPase, and its RNAi mutant contains reduced levels of 16S rRNA and plastid-encoded proteins, suggesting its role in chloroplast ribosome assembly and/or translation (Liu et al. 2010). *Arabidopsis* OBGC, a plant homolog of *E. coli* Obg GTPase, specifically co-precipitates with 23S rRNA in vivo, and *obgc* mutant plants show defective plastid rRNA processing, suggesting that OBGC functions in ribosome biogenesis during chloroplast development (Bang et al. 2012). *Nicotiana benthamiana* DER contains two tandemly repeated GTP-binding domains, and *DER* silencing causes impaired processing of plastid-encoded rRNAs and reduced mRNA translation in chloroplasts (Jeon et al. 2014). Taken together, these results suggest critical functions in chloroplasts for the conserved nuclear-encoded GTPases of prokaryotic origin.

One of the distinct families of the GTPase superfamily is the YlqF/YawG family. A special feature of this family is a circularly permutated arrangement of the GTP-binding motifs. YlqF, later renamed Ribosome Biogenesis GTPase A (RbgA), is essential for cell viability in *Bacillus subtilis* (Uicker et al. 2006). RbgA-depleted *B. subtilis* cells fail to synthesize the mature 50S subunit, but instead accumulate a 45S late assembly intermediate that contains substoichiometric amounts of ribosomal proteins L16, L27, L28, L33a, L35, and L36 (Matsuo et al. 2006; Uicker et al. 2006; Jomaa et al. 2014). RbgA protein is associated with the 45S intermediate in vitro via binding to specific positions in 23S rRNA (Uicker et al. 2006; Matsuo et al. 2006, 2007). Since L16 and L27 are added at a late stage during in vitro 50S ribosome biogenesis in *E. coli*, these results suggest that RbgA participates in a late step of 50S subunit assembly in *B. subtilis*. Recently, screening for suppressors that alleviated the growth defect of a *B. subtilis RbgA* mutant identified independent suppressor strains containing distinct mutations in the ribosomal protein *L6* gene (Gulati et al. 2014). The authors proposed that RbgA facilitates proper interaction between L6 and the maturing 50S ribosome, subsequently triggering the incorporation of the late assembly proteins such as L16, L27, L28, L33a, L35, and L36.

RbgA GTPase homologs are widely distributed in all three kingdoms of life. The *Arabidopsis* genome has seven RbgA homologs: AtRbgA (At4g02790; this study), NSN1 (At3g07050; Jeon et al. 2015), AtNug2 (At1g52980; Im et al. 2011), LSG1-1 (At2g27200) and LSG1-2 (At1g08410) (Weis et al. 2014), SIN2 (At2g41670; Hill et al. 2006), and an uncharacterized GTPase (At4g10650) (Supplementary Fig. 1a). Among these, NSN1 and AtNug2 are targeted to the nucleus/nucleolus, LSG1-1 to the cytosol, LSG1-2 to the nucleus and cytosol, and SIN2 and the At4g10650 protein to the mitochondrion. AtRbgA alone in this family is predicted to be a chloroplast-localized GTPase. NSN1 and *Oryza sativa* Nug2 (OsNug2) are associated with the 60S ribosome, and silencing of *NSN1* and the lack of *OsNug2* complementation on the yeast *nug2* null mutant both result in reduced synthesis of mature 25S rRNA, thus suggesting their roles in biogenesis of the 60S ribosome subunit (Im et al. 2011; Jeon et al. 2015). The *nsn1* null mutants are defective in embryogenesis and leaf and flower development (Wang et al. 2012). Silencing of *NSN1* causes premature senescence in plants, accompanied by induction of senescence marker genes and accumulation of reactive oxygen species (Jeon et al. 2015). LSG1-2, but not LSG1-1, associates with 60S/80S ribosomes, and depletion of LSG1-2 causes accumulation of 18S rRNA precursors without affecting the processing of 25S and 5.8S rRNAs, suggesting that LSG1-2 is involved in 40S maturation (Weis et al. 2014). Finally, *SIN2* encoding a mitochondrial GTPase was identified through genetic screening for *Arabidopsis* mutants with defective ovule development; the *short integuments 2* (*sin2*) mutant produces ovules with short integuments due to cell division defects (Hill et al. 2006). Thus, these RbgA homologs have diverse cellular functions, of which deficiency causes differential effects on plant development.

In this study, we determined the in vivo and in vitro functions of chloroplast-targeted RbgA in higher plants. Plant

RbgA proteins have GTPase activity and are co-fractionated with ribosomes. Virus-induced gene silencing (VIGS) of *NbRbgA* results in defects in rRNA processing and accumulation, polysomal loading of chloroplast mRNAs, and chloroplast protein accumulation. Interestingly, RbgA protein is highly unstable under high light stress. Possible physiological roles of plant RbgA during chloroplast development and stress conditions are discussed.

Materials and methods

Plant materials and growth conditions

Nicotiana benthamiana and *A. thaliana* (ecotype Columbia-0) plants were grown in a growth chamber (23 °C, 100–120 µmol m^{-2} s^{-1} light intensity, and 16 h light/8 h dark cycle). For the high light treatment, *N. benthamiana* leaf disks were floated on liquid 1/2 MS medium and incubated for 1–6 h under high light intensity (1000 µmol m^{-2} s^{-1}).

Virus-induced gene silencing (VIGS)

Tobacco Rattle Virus (TRV)-based VIGS was performed in *N. benthamiana* as described previously (Cho et al. 2013; Jeon et al. 2014, 2015).

Agrobacterium-mediated transient expression

Agrobacterium-mediated transient expression was performed using *Agrobacterium* C58C1 strain as described previously (Ahn et al. 2011; Cho et al. 2013).

BiFC

BiFC was performed using pSPYNE and pSPYCE vectors (Walter et al. 2004). The BiFC constructs were agro-infiltrated into leaves of 3-week-old *N. benthamiana* plants. BiFC signals were monitored 48 h post-infiltration using a confocal laser scanning microscope (Zeiss LSM700).

Real-time quantitative RT-PCR

Total RNA was extracted using the IQeasy™ Plus Plant RNA Extraction Mini Kit (iNtRON Biotechnology). Real-time quantitative RT-PCR was performed as previously described (Ahn et al. 2016) with diluted cDNAs in 96-well plates using SYBR Premix Ex Taq (TAKARA) and the StepOnePlus Real-Time PCR System (Applied Biosystems). Alpha-tubulin mRNA was used as a control for normalization.

RNA gel blot analysis

Total RNA was prepared with TRIzol™ Reagent (Gibco-BRL) following the manufacturer's instructions. RNA gel blot analyses were performed with 20 µg total RNA for each sample as described previously (Jeon et al. 2014). To generate probes, cDNA fragments were PCR-amplified using published sequences and primers as described (Jeon et al. 2014). Probes were labeled using the DecaLabel DNA Labeling Kit (Thermo Scientific).

Immunoblotting

Membrane preparation and immunoblotting were performed according to the manufacturer's instructions using rabbit polyclonal antibodies against rbcL, atpA, atpB, D1, and cpHSP70 (1:10,000, 1:5000, 1:5000, 1:10,000, and 1:10,000 dilution, respectively; Agrisera), and then with horseradish peroxidase-conjugated goat anti-rabbit IgG antibodies (1:5000 dilution; GE Healthcare). Signals were detected by Imagequant LAS 4000 (GE Healthcare Life Sciences). To detect protein expression for BiFC, immunoblotting was performed with mouse monoclonal anti-Myc antibody (1:5000 dilution; CUSABIO) and rat monoclonal anti-HA-Peroxidase antibody (1:5000 dilution; Roche).

Purification of recombinant proteins

The cDNA fragments of NbRbgA, AtRbgA, and their mutants were cloned into the pMAL™c2 vector (New England Biolabs) for MBP fusion. The constructs were transformed into the *E. coli* BL21 strain. The MBP fusion proteins were purified using amylose resin following the manufacturer's instructions (New England Biolabs). After purification, proteins were concentrated using Amicon® Ultracel 30K (Millipore) according to the manufacturer's instructions.

GTPase assay

The turnover rate (k_{cat}) of recombinant proteins of NbRbgA, AtRbgA, and their mutants was measured as described previously (Jeon et al. 2014). A reaction mixture containing 3 µM recombinant proteins and 1 mM GTP in GTPase assay buffer (20 mM Hepes-KOH, pH 8, 1 mM $MgCl_2$, 0.5 mM DTT, and 1 mM NaN_3) was incubated at room temperature for 18 h. The released phosphate was quantified using Biomol green reagent (Biomol Research Laboratories) according to the manufacturer's protocol. The catalytic constant was derived from the equation $k_{cat} = V_{max}/C_{\text{recombinant protein}}$.

Sucrose density gradient sedimentation

GFP-fusion proteins of NbRbgA and its mutants were expressed in *N. benthamiana* leaves by agroinfiltration, and the leaf extracts were subjected to ribosome fractionation as described previously (Cho et al. 2013). The ribosome fractionation protocol consists of two-steps; total ribosomes were first isolated from leaf cell extracts of the VIGS plants, each containing an equal amount of RNA, followed by ribosome fractionation through sucrose density gradients. Proteins extracted from the fractions were separated using SDS-PAGE and subjected to immunoblotting with mouse monoclonal antibodies against GFP (Clontech; 1:5000) and RPL10a (Santa Cruz Biotechnology; 1:5000), and rabbit polyclonal antibody against cpRPL2 (Agrisera; 1:5000). For polysome loading analysis, leaf extracts of the VIGS plants, each containing an equal amount of RNA, were fractionated through 15–55% sucrose density gradients. Total RNA was extracted from the sucrose density gradient fractions and subjected to RNA gel blot analysis.

Results

Identification of plant RbgA

Nicotiana benthamiana RbgA (NbRbgA; Niben-101Scf05559g02012.1; 370 amino acids) and *A. thaliana* RbgA (AtRbgA; At4g02790; 372 amino acids) have a similar protein structure consisting of the N-terminal chloroplast transit peptide (cTP), the conserved GTP-binding domain (GD), and the C-terminal domain (CTD) that has low sequence similarity to known functional proteins (Fig. 1a; Supplementary Fig. 1b). The GTP-binding motifs in the GD are arranged in a circularly permutated order (G4–G1–G2–G3) instead of the normal G1–G2–G3–G4 motif orientation. The GD contains additional conserved regions containing the PGH (Pro-Gly-His) and DAR (Asp-Ala-Arg) motifs. Both the ChloroP algorithm (http://www.cbs.dtu.dk/services/ChloroP/) and the TargetP algorithm (http://www.cbs.dtu.dk/services/TargetP/) identified a chloroplast transit peptide of 72 amino acids at the N-terminus of NbRbgA. Surprisingly, a putative nuclear localization signal (marked by an *asterisk*) was identified within the GD of both NbRbgA and AtRbgA (Fig. 1a; Supplementary Fig. 1b).

RbgA homologs are widely distributed in eukaryotes and prokaryotes (Uicker et al. 2006). Seven RbgA homologs are found in *Arabidopsis*: AtRbgA, NSN1, AtNug2, LSG1-1, LSG1-2, SIN2, and an uncharacterized GTPase (At4g10650). The phylogenetic tree of those homologs revealed that AtRbgA is grouped with the mitochondrial homologs SIN2 and the At4g10650 protein (Supplementary Fig. 1a).

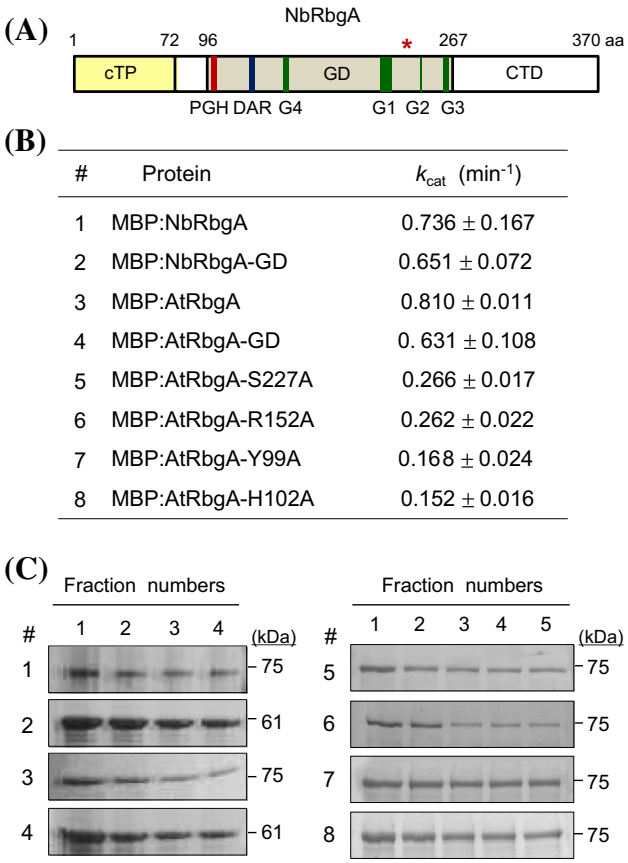

#	Protein	k_{cat} (min^{-1})
1	MBP:NbRbgA	0.736 ± 0.167
2	MBP:NbRbgA-GD	0.651 ± 0.072
3	MBP:AtRbgA	0.810 ± 0.011
4	MBP:AtRbgA-GD	0. 631 ± 0.108
5	MBP:AtRbgA-S227A	0.266 ± 0.017
6	MBP:AtRbgA-R152A	0.262 ± 0.022
7	MBP:AtRbgA-Y99A	0.168 ± 0.024
8	MBP:AtRbgA-H102A	0.152 ± 0.016

Fig. 1 Protein structure and GTPase activity of plant RbgA. **a** Schematic drawing of NbRbgA protein structure. cTP (chloroplast transit peptide; 1 – 72 aa), GD (GTP-binding domain; 96 – 266 aa), and CTD (C-terminal domain; 267 – 370 aa) are marked. The conserved sequences, including the PGH motif, DAR motif, and GTP-binding motifs (G4 – G3) arranged in a circular permutation, are shown. The asterisk indicates the nuclear localization signal. Amino acid (aa) residues are marked. **b** GTPase activities of recombinant NbRbgA, AtRbgA, and their mutants. Values represent means ± standard deviation of triplicate experiments. **c** Purification of MBP fusion proteins of NbRbgA, AtRbgA, and their mutants are shown in **b**. Eluted proteins were visualized by Coomassie staining. After purification, all proteins except MBP:NbRbgA-GD (#2) and MBP:AtRbgA-GD (#4) were further concentrated

Multiple sequence alignment was performed with NbRbgA, AtRbgA, and their homologs from *Oryza sativa* (OsRbgA; Os05g0430400), *Bacillus subtilis* (BsRbgA; NP_389487.1), and *Thermotoga maritima* (TmRbgA/YlqF; Q9WZM6.1) using CLUSTAL-W (Supplementary Fig. 1b). Although prokaryotic RbgA sequences lacked the transit peptide, strong sequence conservation was found in the GD between plant and prokaryotic RbgA proteins, including the G motifs (G4–G1–G2–G3), PGH (Pro-Gly-His) motif, and DAR (Asp-Ala-Arg) motif.

The tertiary structures of NbRbgA and AtRbgA were predicted using an automated homology modeling server [(PS)^2: Protein Structure Prediction Server; http://ps2.life.

nctu.edu.tw/] (Supplementary Fig. 2). The computational model shows that the mature proteins of NbRbgA and AtRbgA are similar to the guanylyl imidodiphosphate-bound form of BsRbgA with respect to overall structure. The N-terminal GTP-binding domain of BsRbgA has the characteristic Rossman fold, while the C-terminal region has multiple α-helices forming a globular α-helical bundle. The C-terminal region of BsRbgA is known to possess RNA-binding activity (Gulati et al. 2013). The ribbon diagram of the conserved GD of plant RbgA almost overlapped with that of BsRbgA, and the CTD also showed a similar topology, despite the limited sequence homology (Supplementary Figs. 1b, 2). The predicted conserved structure of the plant and prokaryotic RbgA suggest a conserved function of these proteins.

GTPase activities of NbRbgA, AtRbgA, and their variants

We determined the GTPase activities of NbRbgA, AtRbgA, and their deletion and site-specific mutants (Fig. 1b, c; Supplementary Fig. 1b). Recombinant proteins of NbRbgA and AtRbgA (lacking the N-terminal chloroplast transit peptide) and their mutant forms were prepared as MBP (maltose binding protein)-fusion proteins (Fig. 1c). The corresponding cDNA fragments were cloned into the pMAL expression vector and expressed in *E. coli*, and the MBP-fusion proteins were affinity-purified using the N-terminal MBP tag, followed by further concentration. At steady state, the kinetic constant (k_{cat}) of NbRbgA and AtRbgA was 0.736 and 0.810 min^{-1}, respectively (Fig. 1b). Previous studies reported that k_{cat} values of *B. subtilis* RbgA, NSN1, and AtNug2 were 0.23, 0.091, and 0.087 min^{-1}, respectively (Im et al. 2011; Achila et al. 2012; Jeon et al. 2015). Repeated experiments suggested that the k_{cat} of NbRbgA and AtRbgA is consistently higher than that of the prokaryotic and plant nuclear RbgA homologs, but lower than the k_{cat} of 1.06 min^{-1} in the NbDER chloroplast GTPase (Jeon et al. 2014). The GTP-binding domains (GD) of NbRbgA and AtRbgA had k_{cat} values of 0.651 and 0.631 min^{-1}, respectively, suggesting that the CTD is not critically important for their in vitro GTPase activity.

Gulati et al. (2013) reported that Lys59 (G4 motif) and Ser134 (G1 motif) were residues crucial for the GTPase activity of *B. subtilis* RbgA, and K59A and S134A mutations caused a severe growth defect. F6A and H9A mutations near and inside the PGH motif also caused significant reduction in GTPase activity and severe growth inhibition, but the R34E mutation in the DAR motif did not affect growth. AtRbgA has the corresponding critical residues, Arg152 (G4 motif), Ser227 (G1 motif), and Tyr99 and His102 (PGH motif), which were mutagenized to alanine (Supplementary Fig. 1b). R152A and S227A mutations in the GD reduced the k_{cat} of AtRbgA to 0.262 and 0.266 min^{-1}, respectively (Fig. 1b). Y99A and H102A mutations in the PGH region more severely affected the GTPase activity by reducing the k_{cat} to 0.168 and 0.152 min^{-1}, respectively. These results suggest that these residues are critical for AtRbgA GTPase activity, and that the chloroplast RbgA protein and the prokaryotic counterpart share structural conservation.

Subcellular localization of plant RbgA

Both NbRbgA and AtRbgA were predicted to have both the chloroplast transit peptide and the nuclear localization signal (Fig. 1a; Supplementary Fig. 1b). To investigate the subcellular localization of NbRbgA and AtRbgA in a plant cell, we expressed GFP fusion proteins in *N. benthamiana* leaves via agroinfiltration under the control of the CaMV35S promoter. Confocal laser scanning microscopy of leaf protoplasts revealed that green fluorescent signals of NbRbgA:GFP and AtRbgA:GFP were mostly detected as distinct particles within chloroplasts (Fig. 2). Infrequently, the signals were detected in both chloroplasts and the nucleus. When the N-terminal region of NbRbgA (Met-1 to Val-80) containing the putative transit peptide was fused with GFP (NbRbgA-N:GFP), the signal was more broadly distributed within the chloroplasts (Fig. 2). Interestingly, the deletion mutant lacking the N-terminal region (NbRbgAΔN:GFP) was mainly targeted to the nucleolus, likely owing to the nuclear localization signal in the GD (Fig. 2; Supplementary Fig. 1b). Collectively, these results suggest that plant RbgA is mainly localized in leaf chloroplasts. However, there is a possibility that plant RbgA proteins may be dual-targeted to chloroplasts and the nucleus under specific developmental or environmental conditions.

Cofractionation of plant RbgA with the ribosomes

NbRbgA and its deletion mutants were expressed as GFP fusion proteins in *N. benthamiana* leaves by agroinfiltration (Fig. 3a). Then the leaf cell extract was fractionated using a sucrose density gradient, and the collected fractions were subjected to immunoblotting with anti-GFP antibodies (Fig. 3a). As the control for fractionation, the same fractions were reacted with antibodies against the chloroplast 50S ribosomal protein L2 (cpRPL2) and the cytosolic 60S ribosomal protein L10a (RPL10a) simultaneously. The cpRPL2 protein is associated with the chloroplast 50S large subunits, 70S monosomes, and polysomes, while RPL10a is associated with the cytosolic 60S large subunits, 80S monosomes, and polysomes. NbRbgA:GFP was mainly detected from the 5th fraction, which is the first fraction containing the 50S/70S ribosomes (marked by the *arrowhead*), to the 8th fraction. NbRbgAΔN:GFP, which lacks the N-terminal region containing the chloroplast transit peptide, was broadly

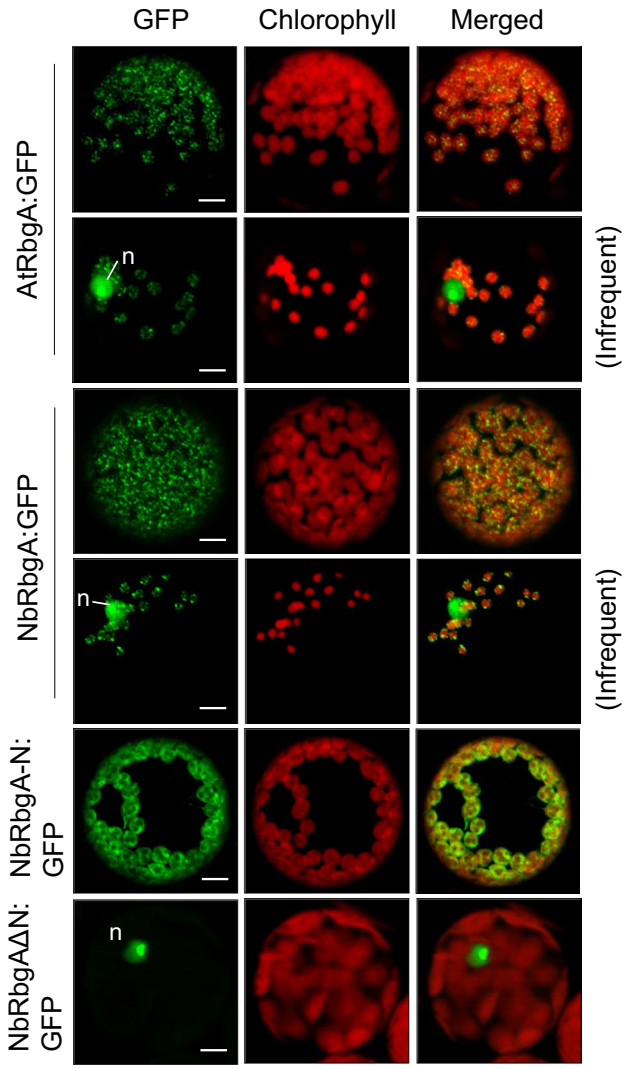

Fig. 2 Subcellular localization of plant RbgA. The full-length AtRbgA (AtRbgA:GFP) and NbRbgA (NbRbgA:GFP), NbRbgA N-terminal region containing the chloroplast transit peptide (NbRbgA-N:GFP), and NbRbgA lacking the N-terminal region (NbRbgAΔN:GFP) were fused to GFP. GFP fusion proteins were expressed in *N. benthamiana* leaves via agroinfiltration. Protoplasts prepared from the infiltrated leaves were observed by confocal laser scanning microscopy for GFP fluorescence and chlorophyll autofluorescence (red). Dual localization of AtRbgA:GFP and NbRbgA:GFP proteins in the nucleus (n) and chloroplasts was infrequently observed. Scale bars 10 μm

distributed in the ribosomal fractions, suggesting a lack of interaction specificity, while CTD:GFP was not incorporated into ribosome fractions. Thus, NbRbgA was co-fractionated primarily with the 50S/70S ribosome in chloroplasts.

Next, to determine whether RbgA interacts with chloroplast ribosomal proteins in planta, we performed bimolecular fluorescence complementation (BiFC). It has been suggested that RbgA facilitates interaction between L6 and the maturing ribosome, which triggers the incorporation of late ribosomal proteins L16, L27, L28, L33, L35, and L36 in *B. subtilis* (Gulati et al. 2014). Furthermore, BsRbgA interacts with L25 in yeast two-hybrid assays, but not with other ribosomal proteins (Matsuo et al. 2006). In *Arabidopsis*, cpRPL6 (At1g05190), cpRPL27 (At5g40950), cpRPL28 (At2g33450), and cpRPL35 (At2g24090) are encoded by the nuclear genome, while cpRPL16 (Atcg00790), cpRPL33 (Atcg00640), and cpRPL36 (Atcg00760) are encoded by the chloroplast genome. Intriguingly, higher plants do not have a chloroplast homolog of prokaryotic RPL25 (Tiller and Bock 2014). Since only the nuclear genes can be tested by BiFC, we performed BiFC with *Arabidopsis* cpRPL6, cpRPL27, cpRPL28, and cpRPL35. AtRbgA and the chloroplast-targeted ribosomal proteins were expressed in combination as yellow fluorescent protein $(YFP)^N$- and YFP^C-fusion proteins in *N. benthamiana* leaves by agroinfiltration. Then, BiFC signals were observed in mesophyll cells of the infiltrated leaves by confocal laser scanning microscopy. Yellow fluorescence within the chloroplasts suggested that AtRbgA interacts with cpRPL6 and cpRPL35 in the chloroplasts (Fig. 3b). Although dual-localization of cpRPL35:GFP in the nucleus and chloroplasts was infrequently observed (Supplementary Fig. 3), the BiFC interaction between AtRbgA and cpRPL35 occurred only in chloroplasts. Yellow fluorescence was not detected with cpRPL27 or cpRPL28, suggesting a lack of interaction despite the high expression of the proteins in the infiltrated leaves (Fig. 3b, c). Since YFP^N and YFP^C are fused to Myc and HA tags, respectively, NbRbgA:YFP^N and cpRPL:YFP^C proteins were detected by immunoblotting using anti-Myc and anti-HA antibodies, respectively.

VIGS phenotypes and reduction of the endogenous *NbRbgA* transcripts

AtRbgA (At4g02790) is a single-copy gene in *Arabidopsis*. According to the SeedGenes Project database (http://www.seedgenes.org/), T-DNA knockout mutants of *AtRbgA* carrying an insertion in the third exon (*emb 3129-1*) or in the second intron (*emb 3129-2*) exhibited an embryonic lethal phenotype. The abnormal embryos were developmentally arrested at the globular stage. Thus, *AtRbgA* is an essential gene for *Arabidopsis* embryo development. To investigate cellular functions of RbgA in plants, we performed virus-induced gene silencing (VIGS) using the tobacco rattle virus (TRV) system against *NbRbgA* in *N. benthamiana* plants (Fig. 4). We cloned three different *NbRbgA* cDNA fragments into the VIGS vector pTV00 and infiltrated *N. benthamiana* plants with *Agrobacterium* containing these plasmids (Fig. 4a). TRV:RbgA(N) and TRV:RbgA(C) contain 556-bp and 554-bp *NbRbgA* cDNA fragments, respectively, whereas TRV:RbgA(F) contains cDNA corresponding to the full-length coding region. VIGS of each construct resulted

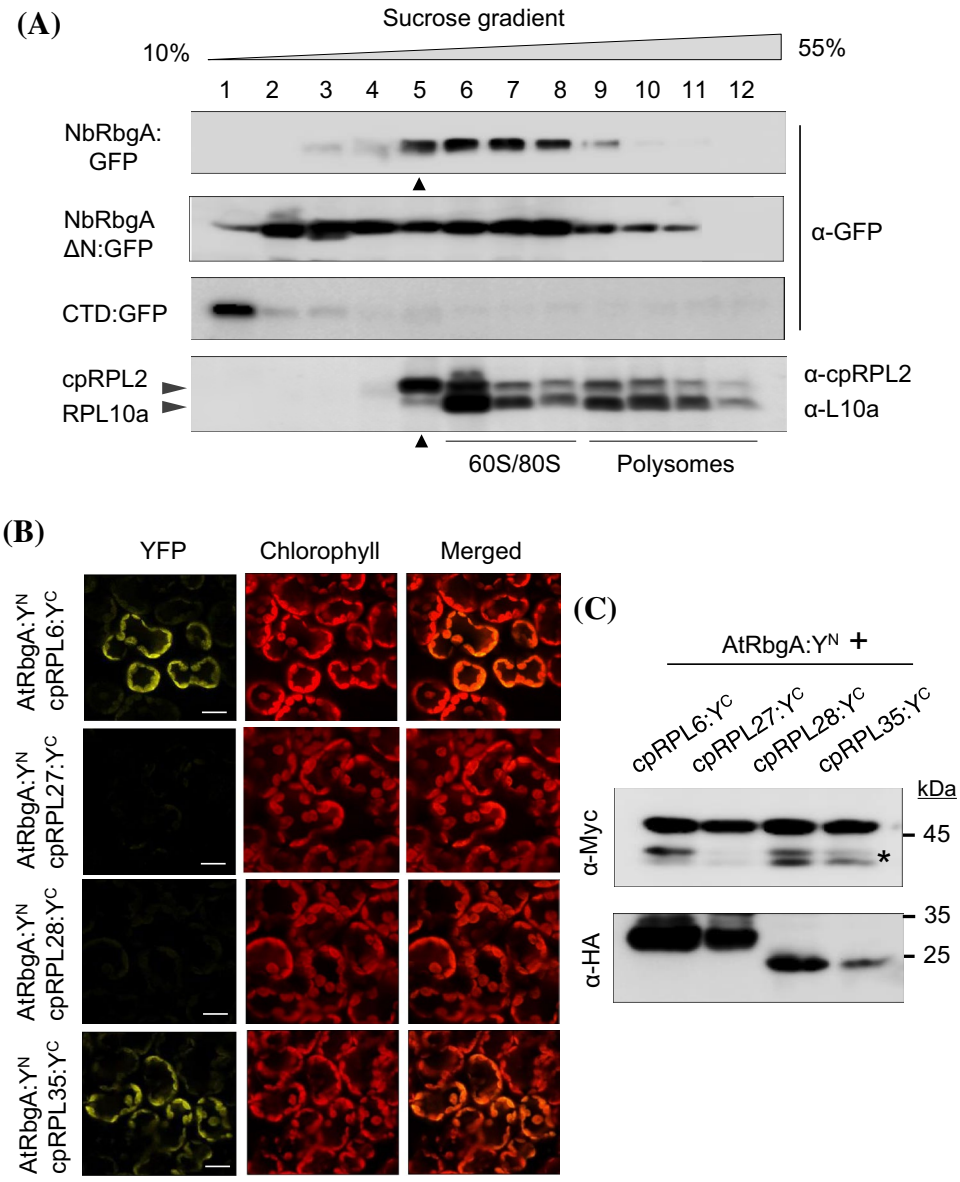

Fig. 3 Association of plant RbgA with chloroplast ribosomes. **a** Sucrose gradient fractionation. NbRbgA and its deletion mutants were expressed in *N. benthamiana* leaves by agroinfiltration. Sucrose density gradient fractions (10–55%) were analyzed by immunoblotting with anti-GFP antibody. As a control, cpRPL2, the chloroplast ribosomal protein, and RPL10a, the eukaryotic ribosomal protein, were detected using immunoblotting with their corresponding antibodies. The first fractions containing NbRbgA:GFP and cpRPL2 are marked by arrowheads. **b** BiFC analyses of AtRbgA interaction with chloroplast ribosomal proteins. Proteins were co-expressed as either YFP^N (Y^N) or YFP^C (Y^C) fusion proteins in *N. benthamiana* leaves using agroinfiltration. Mesophyll cells of the infiltrated leaves were observed for YFP fluorescence using confocal laser scanning microscopy. Scale bars 20 µm. **c** Immunoblotting to determine protein expression in the BiFC experiments shown in **b**. Since YFP^N and YFP^C are fused to Myc and HA tags, respectively, NbRbgA:Y^N and cpRPL:Y^C proteins are detected by anti-Myc and anti-HA antibodies, respectively. The asterisk marks non-specific bands

in a similar leaf-yellowing phenotype, with colors varying from pale-green to yellow/white, accompanied by abnormal leaf morphology (Fig. 4b). To determine the effect of gene silencing, the amount of endogenous *NbRbgA* mRNA in the VIGS plants was measured by real-time quantitative RT-PCR using α-tubulin mRNA as a control (Fig. 4c). The a + b and c + d primers detected reduced amounts of *NbRbgA* mRNA in the yellow sectors of TRV:RbgA(C) and TRV:RbgA(N) leaves, respectively, compared with TRV control, suggesting silencing of *NbRbgA* in these VIGS plants (Fig. 4c).

To observe the effects of *NbRbgA* silencing on chloroplasts, leaf protoplasts prepared from TRV control and the yellow sectors of the TRV:RbgA(N) and TRV:RbgA(C) leaves were visualized by confocal laser scanning microscopy. The chloroplasts in severely affected protoplasts from the *NbRbgA* VIGS plants were much smaller than TRV control chloroplasts (Fig. 4d). The average chlorophyll autofluorescence of protoplasts isolated from TRV:RbgA(N) and TRV:RbgA(C) leaves was reduced to 32–40% of that found in the TRV control (Fig. 4e). These results demonstrate that NbRbgA deficiency impairs chloroplast development. Furthermore, the aberrant chloroplast development appeared to cause stress symptoms in NbRbgA-deficient leaf cells, as shown by a decrease in mitochondrial membrane potential (MMP) and an increase in reactive oxygen species (ROS) (Supplementary Fig. 4a, b). Tetramethylrhodamine methyl ester (TMRM) fluorescent probes accumulate in mitochondria in proportion to MMP (Chazotte 2011). TMRM staining and quantification of the fluorescence suggested that the MMP of TRV:RbgA(N) protoplasts was ~10-fold lower than that of the TRV control (Supplementary Fig. 4a). To

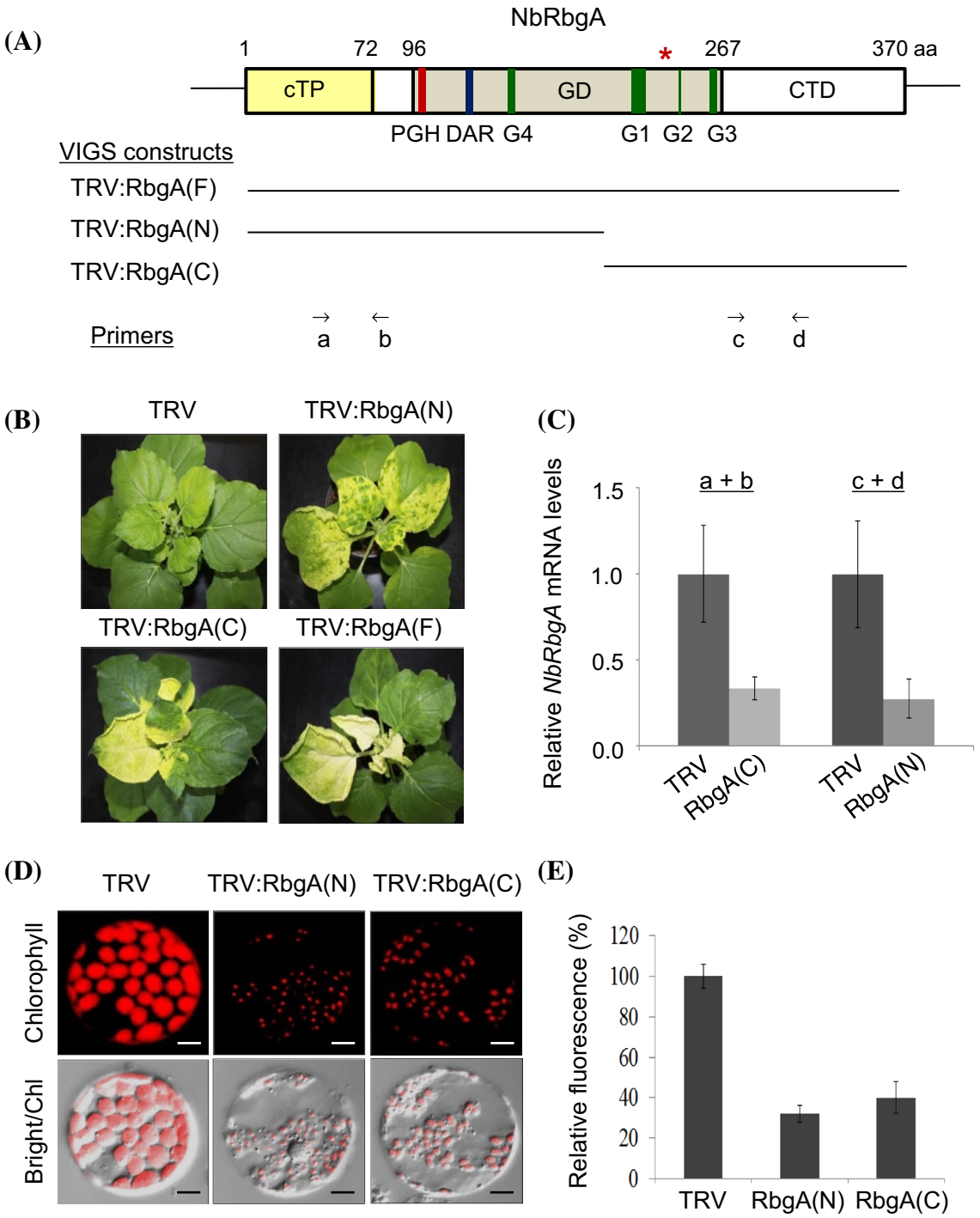

Fig. 4 VIGS phenotypes, endogenous *NbRbgA* transcript levels, and chloroplast defects. **a** Schematic representation of the *NbRbgA* cDNA regions used in the VIGS constructs. The box indicates the protein-coding region of *NbRbgA*. The three VIGS constructs are marked by bars. The positions of primers are indicated. *N. benthamiana* plants were infiltrated with *Agrobacterium* containing the TRV or TRV:RbgA constructs. **b** VIGS phenotypes of the TRV control and three TRV:RbgA VIGS lines. The plants were photographed 20 days after infiltration. **c** Real-time quantitative RT-PCR analyses of the *NbRbgA* transcript levels using the primers shown in **a**. α-tubulin mRNA was used as a control. **d** Chloroplasts in the leaf cells of the VIGS plants were visualized by chlorophyll autofluorescence (Chl) using confocal laser scanning microscopy. TRV:RbgA protoplasts with severe chloroplast defects are shown. Scale bars 10 μm. **e** The average chlorophyll autofluorescence in individual leaf protoplasts was quantified by confocal microscopy. Data points represent means ± standard deviation of 30 individual protoplasts, expressed as a percentage of the TRV control

visualize ROS, the leaf protoplasts were incubated with H_2DCFDA, which becomes activated in the presence of H_2O_2 to produce green fluorescence (Kristiansen et al. 2009). Green fluorescence of TRV:RbgA(N) protoplasts was ~ 14-fold higher than that of the TRV control, suggesting excessive H_2O_2 accumulation (Supplementary Fig. 4b).

Defective protein accumulation in NbRbgA-deficient chloroplasts

Chloroplast protein accumulation in the *RbgA* VIGS plants was examined by immunoblotting using chloroplast HSP70 (cpHSP70), which is encoded by a nuclear gene, as a loading control. Markedly lower levels of plastid-encoded proteins such as atpA and atpB (ATP synthase subunits), D1 (photosystem II core subunit), and rbcL (Rubisco large subunit), were detected in TRV:RbgA(N) and TRV:RbgA(C) plants than in the TRV control (Fig. 5a). To determine whether defective RNA metabolism is responsible for the protein accumulation defect in TRV:RbgA plants, RNA gel blot analysis was performed with 20 µg total RNA for each sample using plastid-encoded genes as probes (Fig. 5b, c). Total rRNAs were stained with ethidium bromide (EtBr) as a control for RNA loading (Fig. 5b). There was no significant difference in the amounts of *psbA, psbD, rbcL, rpoB, atpA, atpB*, and *petB* transcripts in chloroplasts between TRV:RbgA and TRV control leaves (Fig. 5c). Collectively, these results suggest that the reduced accumulation of chloroplast proteins in TRV:RbgA plants is likely caused by a defect in the translational or post-translational steps.

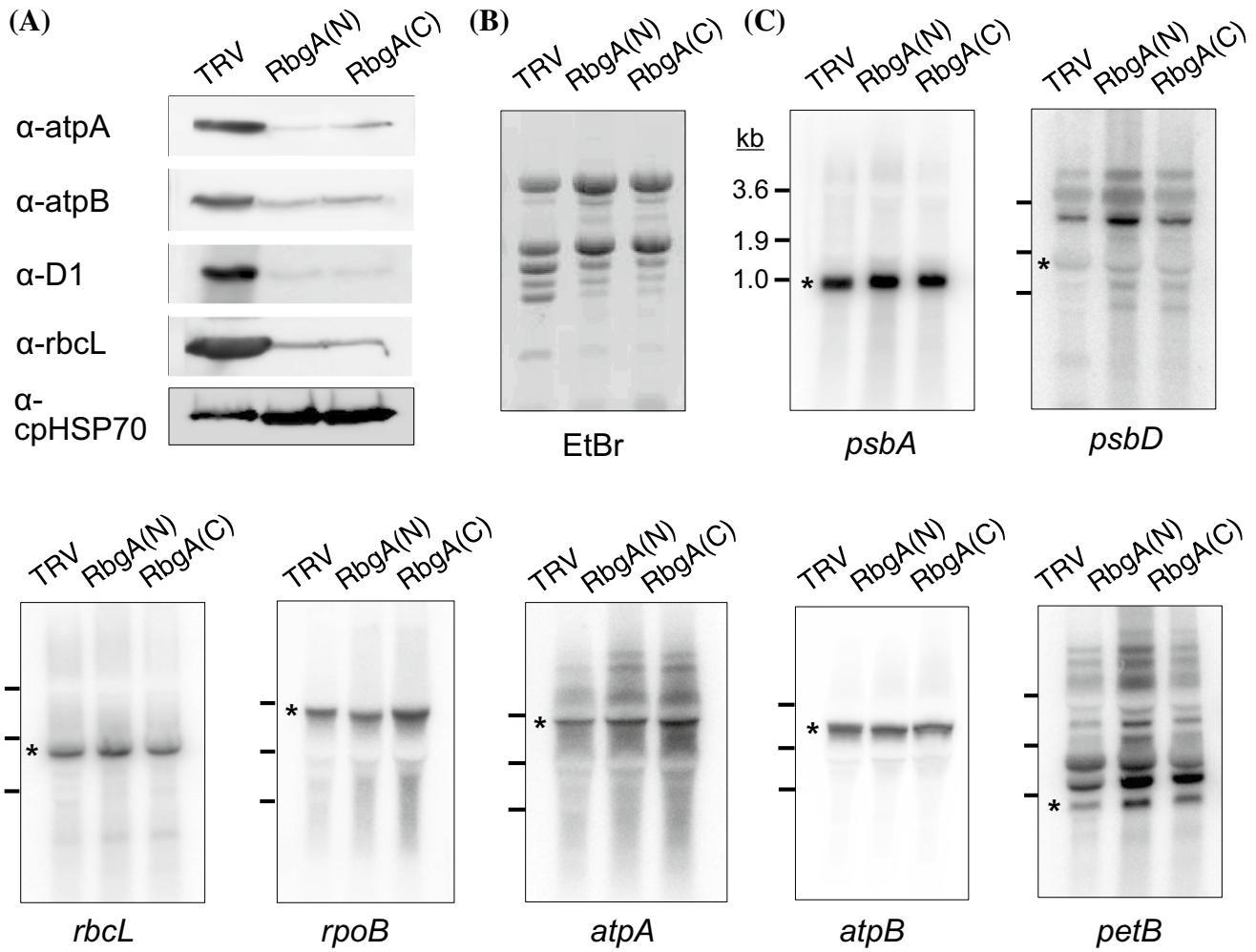

Fig. 5 Protein and mRNA levels of plastid-encoded genes. **a** Immunoblot analyses of chloroplast proteins. Total protein (30 µg) isolated from TRV and TRV:RbgA leaves was subjected to immunoblotting using antibodies against atpA, atpB, D1, and rbcL. As a loading control, chloroplast HSP70 (cpHSP70) was detected by the corresponding antibody. **b, c** Transcript accumulation in chloroplasts. The ethidium bromide (EtBr)-stained gel shows total ribosomal RNAs (**b**). RNA gel blot analysis was performed with total RNA (20 µg per lane) isolated from leaves of TRV and TRV:RbgA VIGS plants (**c**). The bands that match the expected size of the mRNA are marked by asterisks. RNA size markers (3.6-, 1.9-, and 1.0-kb) are indicated in each blot

Defective rRNA accumulation and processing in NbRbgA-deficient chloroplasts

In chloroplasts of higher plants, mature rRNAs are generated via successive processing of a large polycistronic primary transcript produced from the ribosomal RNA (*rrn*) operon (Fig. 6a). The large rRNA precursor form is first processed to generate 16S rRNA, a dicistronic 23S-4.5S rRNA intermediate, and 5S rRNA. Next, processing of the 23S-4.5S intermediate produces the monocistronic 23S and 4.5S rRNAs. The 16S, 23S, and 5S rRNA precursors go through additional processing to generate the mature forms; the 23S rRNA is cleaved into 0.5-, 1.0-, and 1.2-kb mature rRNAs (Kössel et al. 1982; Strittmatter and Kössel 1984).

Since defective rRNA processing is frequently associated with impaired ribosome assembly, we next performed

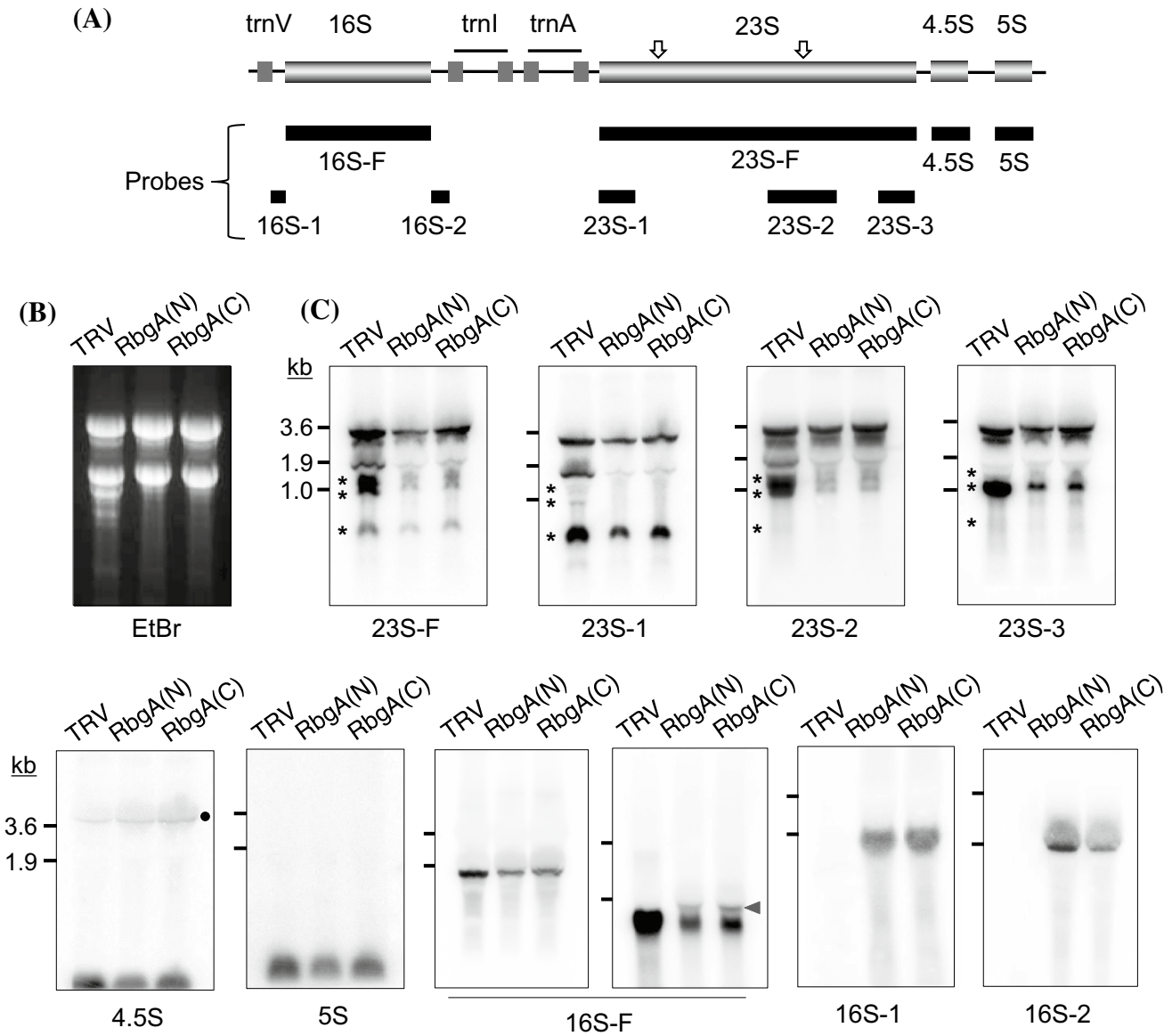

Fig. 6 Accumulation and processing of chloroplast ribosomal RNAs. **a** Schematic representation of the chloroplast *rrn* operon. The rRNA genes (light gray boxes) and the tRNA genes (dark gray boxes) are indicated within the operon. The probes for RNA gel blots are marked by black boxes under the operon. The cleavage sites of 23S rRNA that produce 0.5-kb, 1.0-kb, and 1.2-kb mature rRNAs are marked by white arrows in the operon. **b, c** RNA gel blot analyses of total RNA isolated from TRV, TRV:RbgA(N), and TRV:RbgA(C) leaves. EtBr-stained gels show total ribosomal RNAs (**b**). RNA gel blots (20 µg of total RNA per lane) were hybridized with the different probes shown in **a** (**c**). An additional RNA gel blot is shown for 16S-F probe for better separation of the precursor form of 16S rRNA. The mature forms of 23S rRNA are marked by asterisks. The 23S-4.5S dicistronic processing intermediate is marked by a filled circle. The 16S rRNA precursor forms are marked by an arrowhead. RNA size markers are indicated in each blot

RNA gel blot analyses to investigate chloroplast rRNA processing in the VIGS plants (Fig. 6b, c). EtBr-stained total rRNAs are shown as controls for RNA loading (Fig. 6b). RNA gel blots with 23S-specific probes (Probes 23S-F, 23S-1, 23S-2, and 23S-3) resulted in a complex pattern of RNA bands in the TRV control, which represents both the mature and processing forms of 23S rRNA (Fig. 6c). The final mature forms (0.5-, 1.0-, and 1.2-kb bands) are marked with *asterisks*. TRV:RbgA plants exhibited decreased accumulation of the mature 23S rRNA and defective 23S rRNA processing. The 4.5S probe recognized the mature 4.5S rRNA and small amounts of the 23S-4.5S dicistronic processing intermediate (marked with a *filled circle*). A slight increase in the 23S-4.5S precursor in TRV:RbgA plants suggested a mild defect in the endonucleolytic processing of 4.5S rRNA from the precursor. The 5S probe identified the mature 5S rRNA with no visible accumulation of the precursor forms in the TRV:RbgA plants. Finally, the 16S-F probe detected a reduced amount of mature 16S rRNA and an accumulation of its precursor form (marked with an *arrowhead*) in TRV:RbgA plants (Fig. 6c). The probes 16S-1 and 16S-2 detected the precursor forms in TRV:RbgA plants, suggesting incomplete processing of pre-16S rRNA at both its 5′ and 3′ ends. These results demonstrated that NbRbgA depletion causes pleiotropic defects in chloroplast rRNA processing, and significantly reduces the amounts of mature 23S and 16S rRNAs in chloroplasts.

Reduced polysomal loading of RNA in NbRbgA-deficient chloroplasts

Defective ribosome biogenesis and rRNA processing often affect the polysomal loading of chloroplast RNAs in plants. We examined the association of chloroplast rRNA and mRNA with ribosomes in TRV and TRV:RbgA(N) plants (Fig. 7). Total ribosomes were isolated from leaf cell extracts of the VIGS plants, each containing an equal amount of RNA, and sedimented through a 15–55% sucrose density gradient, and then fractions were collected. RNA gel blot analysis was performed with total RNA purified from each fraction using the 23S and 16S rDNA probes. TRV:RbgA(N) plants contained reduced amounts of 23S and 16S rRNA in the polysomal fractions as compared with the TRV control (Fig. 7a, b). These results suggest that NbRbgA-deficient chloroplasts contain fewer polysomes than TRV chloroplasts, indicative of reduced translation activity in chloroplasts.

Next, polysomal loading of chloroplast-encoded mRNAs *rbcL, psbA*, and *petB* was examined using RNA gel blot analysis with the corresponding probes (Fig. 7c–e). The mRNAs in the polysomal fractions were ribosome-associated mRNAs, undergoing translation. EtBr-staining showed the distribution of total ribosomal RNAs in each fraction (Fig. 7f). Reduced amounts of *rbcL, psbA*, and *petB* mRNAs were present in the polysomal fractions of TRV:RbgA(N) plants, indicating reduced translation of the chloroplast

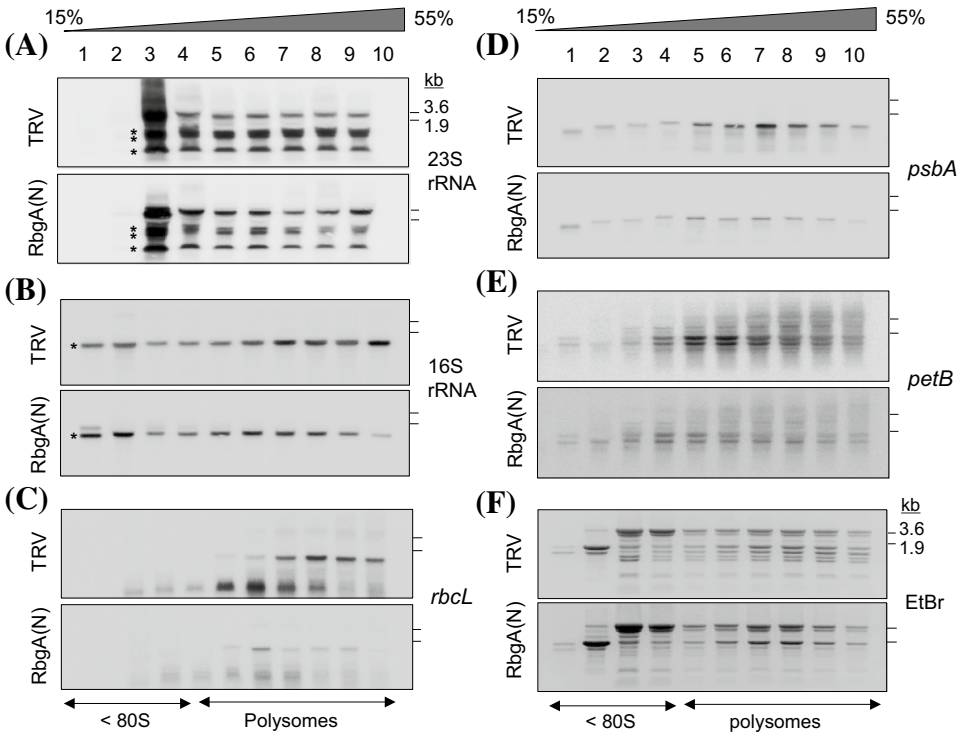

Fig. 7 Polysomal loading of chloroplast RNA. Sucrose density gradient fractions (15–55%) from TRV and TRV:RbgA(N) plants were analyzed by RNA gel blot analysis with 23S rRNA, 16S rRNA, *rbcL, psbA*, and *petB* probes (**a**–**e**); EtBr-staining shows distribution of total ribosomal RNAs in each fraction (**f**). RNA size markers are indicated in each blot. The mature forms of 23S rRNA are marked by asterisks (**a**)

mRNAs. These findings suggest that NbRbgA depletion leads to a decrease in chloroplast translation.

Instability of NbRbgA proteins under high light stress

The stringent response is a survival mechanism of bacteria to cope with stress, which is mediated by the nucleotides guanosine tetraphosphate and pentaphosphate [(p)ppGpp; Dalebroux and Swanson 2012]. It has been recently reported that (p)ppGpp binds to five ribosome biogenesis-related GTPases, including RbgA, to inhibit their activity, leading to inactivation of ribosome assembly under stress conditions (Corrigan et al. 2016). We examined whether NbRbgA proteins become unstable in response to stress conditions in chloroplasts (Fig. 8). NbRbgA:GFP fusion protein was expressed in *N. benthamiana* leaves by agroinfiltration. Leaf disks were prepared from the leaves at 2 days after infiltration, and were then floated on liquid 1/2 MS medium containing cycloheximide (100 μg mL^{-1}) for incubation for 1–6 h under high light intensity (1000 μmol m^{-2} s^{-1}). Since NbRbgA proteins were transiently expressed under the CaMV35S promoter, NbRbgA protein turnover could be monitored using cycloheximide, an inhibitor of cytosolic mRNA translation. The floated leaves did not exhibit any color changes until 6 h of high light treatment. Cell extracts prepared from the leaf disks were subjected to SDS-PAGE and immunoblotting with anti-GFP antibody. As a loading control, the rubisco large subunit (rbcL) was detected using Ponceau S staining. In the presence of cycloheximide, NbRbgA:GFP protein accumulation was dramatically reduced to less than 10% of the control (0 h) after 1 h high light treatment and completely abolished within 2 h (Fig. 8a). High light or cycloheximide alone did not change NbRbgA:GFP protein levels (Fig. 8c). The D1 photosystem II reaction center protein, which is encoded by the chloroplast genome, is a well-known target of photoinhibition; D1 protein is easily degraded under high light conditions (Aro et al. 1993; Nishiyama et al. 2011). Immunoblotting with anti-D1 antibody showed that the endogenous level of D1 protein initially increased until 6 h of high light treatment in the presence of chloramphenicol (CM; 100 μg mL^{-1}), followed by a steep decrease upon longer exposure (Fig. 8b). Chloramphenicol blocks chloroplast protein synthesis (Ellis 1969). These results suggest that the chloroplast NbRbgA protein becomes highly unstable and undergoes rapid degradation under high light stress, and has to be constantly replenished by cytosolic mRNA translation. To examine whether other chloroplast GTPases involved in ribosome biogenesis show similar high light-dependent protein degradation, we expressed NbDER (Jeon et al. 2014) and NbEra (Inoue et al. 2003; Supplementary Fig. 3) as GFP fusion proteins in *N. benthamiana* leaves before exposure to high light for 1–6 h. Accumulation of NbDER and NbEra proteins remained constant under high light conditions up to 6 h in the presence of cycloheximide (Fig. 8a). Furthermore, protein levels of cpRPL28 and cpRPL35 were also constant throughout the treatment (Fig. 8a). Thus, the unusually rapid protein turnover in response to high light appears to be a special feature of NbRbgA.

Excess light produces diverse reactive oxygen species (ROS) in chloroplasts; primarily singlet oxygen ($^1O_2^*$) and H_2O_2 are formed, but superoxide (O_2^-) and hydroxyl radicals ($^*OH$) are also generated (Li et al. 2009). We examined whether NbRbgA:GFP proteins are susceptible to H_2O_2 or methyl viologen (MV), which produces superoxide in chloroplasts (Fig. 8d, e). The leaf disks prepared from the infiltrated leaves were floated for 1–6 h on liquid 1/2 MS media containing 100 mM H_2O_2 or 2 μM MV in the absence or presence of cycloheximide. Immunoblotting showed that NbRbgA:GFP protein levels were constant throughout the 6-h treatment of both chemicals even when cytosolic protein translation was blocked by cycloheximide (Fig. 8d, e). Thus, neither H_2O_2 (100 mM) nor MV (2 μM) was effective at inducing degradation of NbRbgA:GFP proteins in chloroplasts.

Discussion

The RbgA family of GTPases, which has a circularly permutated arrangement of the GTP-binding motifs, modulates diverse aspects of plant growth and development through differential subcellular localizations, activities, and functions (Hill et al. 2006; Im et al. 2011; Weis et al. 2014; Jeon et al. 2015). In this study, we investigated the characteristics and functions of the unique chloroplast-targeted RbgA homolog. NbRbgA and AtRbgA exhibit conserved protein sequences and structural conformation as compared with their prokaryotic counterparts such as *B. subtilis* RbgA and *T. maritima* YlqF/RbgA (Supplementary Figs. 1, 2). The conserved sequence residues shared between plant and bacterial RbgA proteins include the GTP-binding motifs, PGH motif, and DAR motif. However, their CTDs show low sequence similarity. Gulati et al. (2013) performed extensive mutagenesis in *B. subtilis* RbgA (BsRbgA) to gain insight into the ribosome interaction and GTPase activation of RbgA. They identified essential residues in the conserved region 1 (CR1) containing the PGH motif, the GTP-binding motifs, and the CTD, but mutations in CR2 containing the DAR motif caused only a minor defect in cell growth and BsRbgA GTPase activity. In our study, the S227A (G1) and S152A (G4) mutations reduced AtRbgA GTPase activity to 33 and 32% of the control, respectively, suggesting the importance of the G1 and G4 motifs for this activity (Fig. 1). Furthermore, the Y99A and H102A mutations affecting the PGH motif region resulted in a severe reduction in the

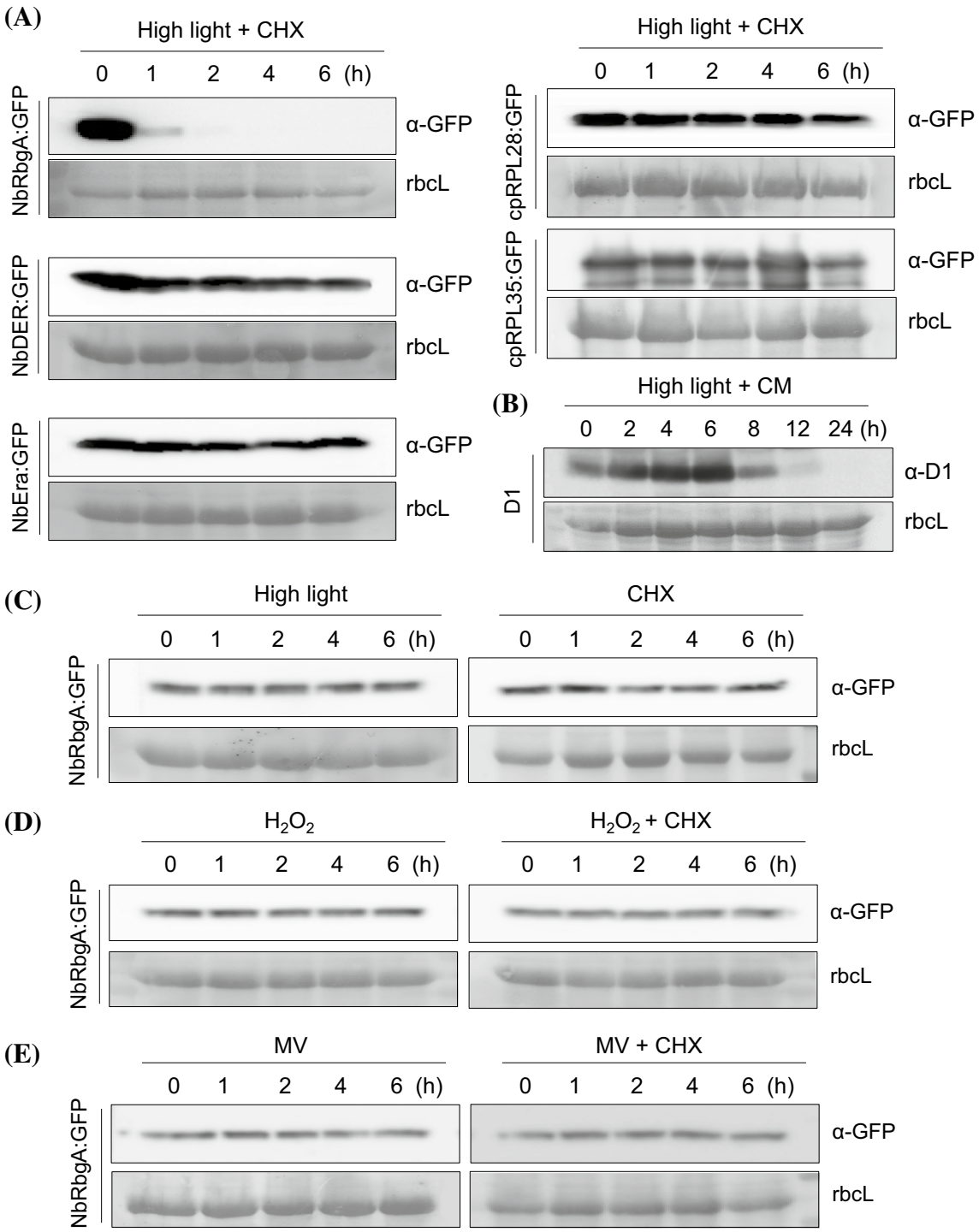

Fig. 8 Instability of RbgA proteins under high light stress conditions. **a** NbRbgA:GFP and other GFP fusion proteins were expressed in *N. benthamiana* leaves by agroinfiltration. Leaf disks prepared from the infiltrated leaves were floated on liquid 1/2 MS medium containing cycloheximide (CHX; 100 μg mL^{-1}), and incubated under high light conditions (1000 μmol m^{-2} s^{-1}) for 1–6 h. Protein extracts isolated from the leaf disks after high light treatment were subjected to immunoblotting using anti-GFP antibody. As a loading control, the rubisco large subunit (rbcL) was detected using Ponceau S staining. **b** Endogenous levels of D1 photosystem II reaction center protein were examined by immunoblotting with anti-D1 antibody. Leaf disks were floated on liquid 1/2 MS medium containing chloramphenicol (CM; 100 μg mL^{-1}), and incubated under high light conditions (1000 μmol m^{-2} s^{-1}) for 2–24 h. **c** Leaf disks expressing NbRbgA:GFP were treated with high light or CHX alone for 1–6 h. **d** Leaf disks expressing NbRbgA:GFP were treated with 100 mM H_2O_2 in the absence or presence of CHX for 1–6 h. **e** Leaf disks expressing NbRbgA:GFP were treated with 2 μM methyl viologen (MV) in the absence or presence of CHX for 1–6 h

intrinsic GTPase activity of AtRbgA. These results are consistent with the mutagenic effects on the corresponding residues of BsRbgA (Gulati et al. 2013). The PGH motif is conserved in almost all EF-Tu (elongation factor thermo unstable) homologs, and His84 of EF-Tu GTPase as part of the PGH motif is essential for GTP hydrolysis (Daviter et al. 2003). An alignment of crystal structures of BsRbgA and EF-Tu suggests that His9 from the PGH motif of BsRbgA is localized in a similar position to that of the catalytic His84 of EF-Tu, suggesting that His9 acts as a catalytic His residue (Gulati et al. 2013). A difference is that His84 is localized in the G3 region of EF-Tu, while His9 is found in the highly flexible CR1 region at the N-terminus of BsRbgA. Among the seven RbgA homologs in *Arabidopsis*, only three organellar RbgA homologs (AtRbgA, SIN2, and At4g10650 protein) have the PGH motif at the N-terminus of the protein, while the other eukaryotic RbgA homologs lack the motif. Collectively, these results suggest that the His residue in the PGH motif of AtRbgA and of other organellar homologs may play a role as the catalytic His for GTPase activity.

The predicted overall protein structures of AtRbgA and NbRbgA are very similar to that of BsRbgA; even the CTD structure is conserved despite low sequence similarity (Supplementary Figs. 1b, 2). The CTDs of these three proteins show a three α-helical arrangement that is topologically similar to that of the ANTAR domain (Shu and Zhulin 2002; Gulati et al. 2013). ANTAR is an RNA-binding domain found in transcription antitermination regulatory proteins such as AmiR and NasR (Shu and Zhulin 2002). BsRbgA binds to 23S rRNA of the 50S subunit (Matsuo et al. 2006), and mutations in the CTD disrupt BsRbgA binding to the 50S ribosome (Gulati et al. 2013). These results suggest a possible involvement of the CTD of chloroplast RbgA in the interaction with the 50S subunit.

Ribosome biogenesis is a complex and tightly coordinated process that involves the synthesis, processing, and chemical modification of rRNAs, ordered assembly of the ribosomal components, and maturation. Numerous biogenesis factors, including endo- and exo-ribonucleases, RNA helicases, RNA modification enzymes, chaperones, and GTPases, participate in prokaryotic and eukaryotic ribosome assembly (Woolford and Baserga 2013). RbgA is an essential ribosome-associated GTPase that plays a critical role in a late step of the 50S ribosome biogenesis in *B. subtilis* (Matsuo et al. 2006, 2007; Uicker et al. 2006). RbgA depletion in *B. subtilis* leads to accumulation of a 45S late assembly intermediate that contains severely reduced amounts of ribosomal proteins L16, L27, L28, L33, L35, and L36 (Li et al. 2013; Jomaa et al. 2014). L16 and L27 are critical components of the peptidyltransferase center in the 50S subunit that play a role in stabilization of the peptide bond formation and tRNA positioning on the A- and P-sites (Wekselman et al. 2009; Gulati et al. 2014). Incorporation of L16, occurring at a late stage in the in vitro 50S assembly process in *E. coli*, stimulates GTPase activity of BsRbgA and induces the release of this factor for the conversion of the 45S intermediate to the mature 50S subunit (Jomaa et al. 2014). Furthermore, the yeast eukaryotic RbgA homolog LSG1p may modulate the incorporation of the L16 homolog Rpl10 into the 60S large subunit (Hedges et al. 2005). Recent studies have suggested that RbgA facilitates the incorporation of L16 and other late ribosomal proteins through proper positioning of L6 on the maturing ribosome or through structural remodeling of rRNAs using its RNA chaperone activity (Gulati et al. 2014; Li et al. 2013).

In plants, eukaryotic RbgA homologs such as NSN1 and AtNug2 have been implicated in assembly of the 60S ribosomal subunit (Im et al. 2011; Jeon et al. 2015), while another homolog, LSG1-2, binds to the 60S subunit but modulates 40S maturation, suggesting that 60S subunit maturation is important for the final steps of 40S maturation (Weis et al. 2014). Mutations that affect chloroplast ribosome assembly frequently result in rRNA processing defects, and the final maturation of the chloroplast 23S rRNA appears to occur after ribosome assembly (Bellaoui et al. 2003; Bollenbach et al. 2005). In this study, chloroplast-targeted NbRbgA was mainly co-fractionated with 50S/70S ribosomes in sucrose density gradient sedimentation (Fig. 3a), and AtRbgA was found to interact with cpRPL6 and cpRPL35 (Fig. 3b). Furthermore, NbRbgA depletion led to reduced accumulation of mature 23S and 16S rRNAs, caused rRNA processing defects, and decreased polysomal loading of plastid-encoded mRNAs (Figs. 6c, 7), suggesting a role for NbRbgA in chloroplast ribosome biogenesis. Defective rRNA processing and/or ribosome assembly in NbRbgA-deficient chloroplasts might have triggered degradation of the rRNAs. Although molecular mechanisms of chloroplast RbgA function still remain elusive, there is a possibility that it plays a role in recruiting ribosomal proteins at a late stage of chloroplast ribosome assembly, similar to the actions of BsRbgA and yeast LSG1p (Hedges et al. 2005; Jomaa et al. 2014). BsRbgA interacts with RPL25 (Matsuo et al. 2007), and is functionally linked to RPL6; BsRbgA regulates correct positioning of L6 on the maturing ribosome prior to the incorporation of L16 and other late assembly proteins (Gulati et al. 2014). In this study, AtRbgA was found to interact with cpRPL6 and cpRPL35 (Fig. 3b). Both cpRPL6 and cpRPL35 are essential for *Arabidopsis* embryogenesis at the globular stage when pro-plastids start to differentiate into chloroplasts (http://www.seedgenes.org/; Romani et al. 2012). Plant RbgA may operate through cpRPL6 during chloroplast 50S ribosome biogenesis, mimicking the BsRbgA action during prokaryotic 50S ribosome biogenesis. However, RbgA interaction with cpRPL35 (Fig. 3b) and the lack of a chloroplast homolog of RPL25 in higher plants (Tiller and Bock 2014) suggest that details of chloroplast RbgA action may

differ from those of its bacterial counterparts during ribosome biogenesis.

Many ribosome-associated GTPases, including RbgA, participate in the late stages of the biogenesis process in prokaryotes (Britton 2009; Verstraeten et al. 2011). It has been proposed that these GTPases modulate the ribosome assembly rate according to cellular guanine nucleotide concentrations; low cellular GTP levels caused by nutrient/energy deficiency would inactivate the GTPases, shutting down further ribosome assembly (Britton 2009; Jomaa et al. 2014). Interestingly, we observed that NbRbgA shows a high turnover rate during high light stress (Fig. 8a). The phenomenon, however, was not observed with NbDER GTPase involved in chloroplast ribosome biogenesis (Jeon et al. 2014) or with chloroplast ribosomal proteins such as cpRPL28 or cpRPL35. Photo-oxidative stresses can cause oxidation of amino acid residues, particularly methionine and cysteine, leading to protein destabilization and denaturation (Berlett and Stadtman 1997; Stadtman 2006). NbRbgA appears to be susceptible to photo-oxidation, which causes protein denaturation and subsequent degradation by chloroplast proteases. Interestingly, neither H_2O_2 nor MV treatment stimulated degradation of NbRbgA (Fig. 8d, e), although both treatments are known to cause damages to photosystem (PS) II. Production of singlet oxygen ($^1O_2$) mainly occurs in chloroplasts from the interaction of chlorophyll triplet excited stages (^{3}Chl*) with oxygen (Triantaphylidès and Havaux 2009). $^1O_2$ production seems to be associated with excess photosynthetically active radiation, but not with UV-B, cold stress, or MV (Hideg et al. 2000). Furthermore, $^1O_2$ is the main ROS involved in photo-oxidative damage to plants (Triantaphylidès et al. 2008). Collectively, our results suggest that NbRbgA proteins in chloroplasts may be particularly susceptible to $^1O_2$-induced photo-oxidation.

PSII is sensitive to photoinhibition under excess light conditions, and the primary target of photoinhibition is the PSII reaction center D1 protein; the half-life of D1 is inversely correlated with light intensity (Aro et al. 1993; Takahashi and Murata 2008). To repair the damaged PSII, the inactivated D1 protein must be degraded, de novo synthesized, and incorporated into the reaction center (Edelman and Mattoo 2008). Evidence shows that global mRNA translation in chloroplasts, including that of the *psbA2* mRNA that encodes D1, is markedly repressed during photoinhibition, suggesting that the translation machinery may be a target of inactivation by ROS (Nishiyama et al. 2006, 2011). In particular, translation elongation factor G (EF-G) was shown to be susceptible to oxidation in cyanobacteria; the oxidation of two specific cysteine residues was the main cause of EF-G inactivation (Kojima et al. 2009). The rapid turnover of RbgA under high light conditions suggests that RbgA may be a target of photoinhibition in chloroplasts. NbRbgA GTPase activity and high turnover rate may contribute to rapid inhibition of chloroplast ribosome biogenesis under high light stress.

Acknowledgements This research was supported by the Cooperative Research Program for Agriculture Science & Technology Development [Project Numbers PJ01118901 (Systems & Synthetic Agrobiotech Center) and PJ01114701 (Plant Molecular Breeding Center)] from the Rural Development Administration (to H.-S. Pai), and the Basic Science Research Program (Project Number 2016-11-1224) from the National Research Foundation of Republic of Korea (to Y. Jeon).

Author contributions Y.J. performed all of the experiments with the help of H.-K.A and Y.W.K. Y.J. and H.-S.P. designed the experiments, discussed the results, and wrote the manuscript.

Compliance with ethical standards

Conflict of interest The authors declare that they have no conflict of interest.

References

Achila D, Gulati M, Jain N, Britton RA (2012) Biochemical characterization of ribosome assembly GTPase RbgA in *Bacillus subtilis*. J Biol Chem 287:8417–8423

Adilakshmi T, Bellur DL, Woodson SA (2008) Concurrent nucleation of 16S folding and induced fit in 30S ribosome assembly. Nature 455:1268–1272

Ahmed T, Yin Z, Bhushan S (2016) Cryo-EM structure of the large subunit of the spinach chloroplast ribosome. Sci Rep 6:35793

Ahn CS, Han J-A, Lee H-S, Lee S, Pai H-S (2011) The PP2A regulatory subunit Tap46, a component of TOR signaling pathway, modulates growth and metabolism in plants. Plant Cell 23:185–209

Ahn CS, Cho HK, Lee D-H, Sim H-J, Kim S-G, Pai H-S (2016) Functional characterization of the ribosome biogenesis factors PES, BOP1, and WDR12 (PeBoW), and mechanisms of defective cell growth and proliferation caused by PeBoW deficiency in *Arabidopsis*. J Exp Bot 67:5217–5232

Aro EM, Virgin I, Andersson B (1993) Photoinhibition of photosystem II. Inactivation, protein damage and turnover. Biochim Biophys Acta 1143:113–134

Bang WY, Chen J, Jeong IS, Kim SW, Kim CW, Jung HS, Lee KH, Kweon HS, Yoko I, Shiina T, Bahk JD (2012) Functional characterization of ObgC in ribosome biogenesis during chloroplast development. Plant J 71:122–134

Bellaoui M, Keddie JS, Gruissem W (2003) DCL is a plant-specific protein required for plastid ribosomal RNA processing and embryo development. Plant Mol Biol 53:531–543

Berlett BS, Stadtman ER (1997) Protein oxidation in aging, disease, and oxidative stress. J Biol Chem 272:20313–20316

Bollenbach TJ, Lange H, Gutierrez R, Erhardt M, Stern DB, Gagliardi D (2005) RNR1, a 3′-5′ exoribonuclease belonging to the RNR superfamily, catalyzes 3′ maturation of chloroplast ribosomal RNAs in *Arabidopsis thaliana*. Nucleic Acids Res 33:2751–2763

Britton RA (2009) Role of GTPases in bacterial ribosome assembly. Annu Rev Microbiol 63:155–176

Caldon CE, March PE (2003) Function of the universally conserved bacterial GTPases. Curr Opin Microbiol 6:135–139

Chazotte B (2011) Labeling mitochondria with TMRM or TMRE. Cold Spring Harb Protoc 2011:895–897

Cho HK, Ahn CS, Lee H-S, Kim J-K, Pai HS (2013) Pescadillo plays an essential role in plant cell growth and survival by modulating ribosome biogenesis. Plant J 76:393–405

Corrigan RM, Bellows LE, Wood A, Gründling A (2016) ppGpp negatively impacts ribosome assembly affecting growth and antimicrobial tolerance in Gram-positive bacteria. Proc Natl Acad Sci USA 113:E1710–E1719

Dalebroux ZD, Swanson MS (2012) ppGpp: magic beyond RNA polymerase. Nature Rev Microbiol 10:203–212

Daviter T, Wieden HJ, Rodnina MV (2003) Essential role of histidine 84 in elongation factor Tu for the chemical step of GTP hydrolysis on the ribosome. J Mol Biol 332:689–699

Edelman M, Mattoo AK (2008) D1-protein dynamics in photosystem II: the lingering enigma. Photosynth Res 98:609–620

Ellis RJ (1969) Chloroplast ribosomes: stereospecificity of inhibition by chloramphenicol. Science 163:477–478

Gulati M, Jain N, Anand B, Prakash B, Britton RA (2013) Mutational analysis of the ribosome assembly GTPase RbgA provides insight into ribosome interaction and ribosome-stimulated GTPase activation. Nucleic Acids Res 41:3217–3227

Gulati M, Jain N, Davis JH, Williamson JR, Britton RA (2014) Functional interaction between ribosomal protein L6 and RbgA during ribosome assembly. PLoS Genet 10:e1004694

Hedges J, West M, Johnson AW (2005) Release of the export adapter, Nmd3p, from the 60S ribosomal subunit requires Rpl10p and the cytoplasmic GTPase Lsg1p. EMBO J 24:567–579

Herold M, Nierhaus KH (1987) Incorporation of six additional proteins to complete the assembly map of the 50S subunit from *Escherichia coli* ribosomes. J Biol Chem 262:8826–8833

Hideg E, Kálai T, Hideg K, Vass I (2000) Do oxidative stress conditions impairing photosynthesis in the light manifest as photoinhibition? Philos Trans R Soc Lond B Biol Sci 355:1511–1516

Hill TA, Broadhvest J, Kuzoff RK, Gasser CS (2006) *Arabidopsis* SHORT INTEGUMENTS 2 is a mitochondrial DAR GTPase. Genetics 174:707–718

Im CH, Hwang SM, Son YS, Heo JB, Bang WY, Suwastika IN, Shiina T, Bahk JD (2011) Nuclear/nucleolar GTPase 2 proteins as a subfamily of YlqF/YawG GTPases function in pre-60S ribosomal subunit maturation of mono- and dicotyledonous plants. J Biol Chem 286:8620–8632

Inoue K, Alsina J, Chen J, Inouye M (2003) Suppression of defective ribosome assembly in a rbfA deletion mutant by overexpression of Era, an essential GTPase in *Escherichia coli*. Mol Microbiol 48:1005–1016

Jeon Y, Ahn CS, Jung HJ, Kang H, Park GT, Choi Y, Hwang J, Pai HS (2014) DER containing two consecutive GTP-binding domains plays an essential role in chloroplast ribosomal RNA processing and ribosome biogenesis in higher plants. J Exp Bot 65:117–130

Jeon Y, Park YJ, Cho HK, Jung HJ, Ahn TK, Kang H, Pai HS (2015) The nucleolar GTPase nucleostemin-like 1 plays a role in plant growth and senescence by modulating ribosome biogenesis. J Exp Bot 66:6297–6310

Jomaa A, Jain N, Davis JH, Williamson JR, Britton RA, Ortega J (2014) Functional domains of the 50S subunit mature late in the assembly process. Nucleic Acids Res 42:3419–3435

Kojima K, Motohashi K, Morota T, Oshita M, Hisabori T, Hayashi H, Nishiyama Y (2009) Regulation of translation by the redox state of elongation factor G in the cyanobacterium *Synechocystis* sp. PCC 6803. J Biol Chem 284:18685–18691

Kössel H, Edwards K, Koch W, Langridge P, Schiefermayr E, Schwarz Z, Strittmatter G, Zenke G (1982) Structural and functional analysis of an rRNA operon and its flanking tRNA genes from *Zea mays* chloroplasts. Nucleic Acids Symp Ser 11:117–120

Kristiansen KA, Jensen PE, Møller IM, Schulz A (2009) Monitoring reactive oxygen species formation and localisation in living cells by use of the fluorescent probe CM-H_2DCFDA and confocal laser microscopy. Physiol Plant 136:369–383

Li Z, Wakao S, Fischer BB, Niyogi KK (2009) Sensing and responding to excess light. Annu Rev Plant Biol 60:239–260

Li N, Chen Y, Guo Q, Zhang Y, Yuan Y, Ma C, Deng H, Lei J, Gao N (2013) Cryo-EM structures of the late-stage assembly intermediates of the bacterial 50S ribosomal subunit. Nucleic Acids Res 41:7073–7083

Liu H, Lau E, Lam MP et al (2010) OsNOA1/RIF1 is a functional homolog of AtNOA1/RIF1: implication for a highly conserved plant cGTPase essential for chloroplast function. New Phytol 187:83–105

Manuell AL, Quispe J, Mayfield SP (2007) Structure of the chloroplast ribosome: novel domains for translation regulation. PLoS Biol 5:e209

Matsuo Y, Morimoto T, Kuwano M, Loh PC, Oshima T, Ogasawara N (2006) The GTP-binding protein YlqF participates in the late step of 50 S ribosomal subunit assembly in *Bacillus subtilis*. J Biol Chem 281:8110–8117

Matsuo Y, Oshima T, Loh PC, Morimoto T, Ogasawara N (2007) Isolation and characterization of a dominant negative mutant of *Bacillus subtilis* GTP-binding protein, YlqF, essential for biogenesis and maintenance of the 50 S ribosomal subunit. J Biol Chem 282:25270–25277

Nishiyama Y, Allakhverdiev SI, Murata N (2006) A new paradigm for the action of reactive oxygen species in the photoinhibition of photosystem II. Biochim Biophys Acta 1757:742–749

Nishiyama Y, Allakhverdiev SI, Murata N (2011) Protein synthesis is the primary target of reactive oxygen species in the photoinhibition of photosystem II. Physiol Plant 142:35–46

Röhl R, Nierhaus KH (1982) Assembly map of the large subunit (50S) of *Escherichia coli* ribosomes. Proc Natl Acad Sci USA 79:729–733

Romani I, Tadini L, Rossi F, Masiero S, Pribil M, Jahns P, Kater M, Leister D, Pesaresi P (2012) Versatile roles of Arabidopsis plastid ribosomal proteins in plant growth and development. Plant J 72:922–934

Sharma MR, Wilson DN, Datta PP, Barat C, Schluenzen F, Fucini P, Agrawal RK (2007) Cryo-EM study of the spinach chloroplast ribosome reveals the structural and functional roles of plastid-specific ribosomal proteins. Proc Natl Acad Sci USA 104:19315–19320

Shu CJ, Zhulin IB (2002) ANTAR: an RNA-binding domain in transcription antitermination regulatory proteins. Trends Biochem Sci 27:3–5

Stadtman ER (2006) Protein oxidation and aging. Free Radic Res 40:1250–1258

Strittmatter G, Kössel H (1984) Cotranscription and processing of 23S, 4.5S and 5S rRNA in chloroplasts from *Zea mays*. Nucleic Acids Res 12:7633–7647

Sykes MT, Williamson JR (2009) A complex assembly landscape for the 30S ribosomal subunit. Annu Rev Biophys 38:197–215

Takahashi S, Murata N (2008) How do environmental stresses accelerate photoinhibition? Trends Plant Sci 13:178–182

Talkington MW, Siuzdak G, Williamson JR (2005) An assembly landscape for the 30S ribosomal subunit. Nature 438:628–632

Tiller N, Bock R (2014) The translational apparatus of plastids and its role in plant development. Mol Plant 7:1105–1120

Traub P, Nomura M (1968) Structure and function of *E. coli* ribosomes. V. Reconstitution of functionally active 30S ribosomal particles from RNA and proteins. Proc Natl Acad Sci USA 59:777–784

Traub P, Nomura M (1969) Structure and function of *Escherichia coli* ribosomes. VI. Mechanism of assembly of 30 s ribosomes studied *in vitro*. J Mol Biol 40:391–413

Triantaphylidès C, Havaux M (2009) Singlet oxygen in plants: production, detoxification and signaling. Trends Plant Sci 14:219–228

Triantaphylidès C, Krischke M, Hoeberichts FA, Ksas B, Gresser G, Havaux M, Van Breusegem F, Mueller MJ (2008) Singlet oxygen is the major reactive oxygen species involved in photooxidative damage to plants. Plant Physiol 148:960–968

Uicker WC, Schaefer L, Britton RA (2006) The essential GTPase RbgA (YlqF) is required for 50S ribosome assembly in *Bacillus subtilis*. Mol Microbiol 59:528–540

Verstraeten N, Fauvart M, Versées W, Michiels J (2011) The universally conserved prokaryotic GTPases. Microbiol Mol Biol Rev 75:507–542

Walter M, Chaban C, Schütze K et al (2004) Visualization of protein interactions in living plant cells using bimolecular fluorescence complementation. Plant J 40:428–438

Wang X, Gingrich DK, Deng Y, Hong Z (2012) A nucleostemin-like GTPase required for normal apical and floral meristem development in *Arabidopsis*. Mol Biol Cell 23:1446–1456

Weis BL, Missbach S, Marzi J, Bohnsack MT, Schleiff E (2014) The 60S associated ribosome biogenesis factor LSG1-2 is required for 40S maturation in *Arabidopsis thaliana*. Plant J 280:1043–1056

Wekselman I, Davidovich C, Agmon I, Zimmerman E, Rozenberg H, Bashan A, Berisio R, Yonath A (2009) Ribosome's mode of function: myths, facts and recent results. J Pept Sci 15:122–130

Woolford JL Jr, Baserga SJ (2013) Ribosome biogenesis in the yeast *Saccharomyces cerevisiae*. Genetics 195:643–681

Yamaguchi K, Subramanian AR (2000) The plastid ribosomal proteins: identification of all the proteins in the 50S subunit of an organelle ribosome (chloroplast). J Biol Chem 275:28466–28482

Yamaguchi K, Subramanian AR (2003) Proteomic identification of all plastid-specific ribosomal proteins in higher plant chloroplast 30S ribosomal subunit. Eur J Biochem 270:190–205